EEET ECOLOGICAL ENGINEERING & ENVIRONMENTAL TECHNOLOGY

Ecological Engineering & Environmental Technology, 2026, 27(12), 437–458
https://doi.org/10.12912/27197050/241777
ISSN 2719–7050, License CC-BY 4.0

Received: 2026.09.18
Accepted: 2026.10.20
Published: 2026.11.02

Development of an integrated production system for microalgae-based agricultural biostimulant

Karina Rodríguez-Mora[1,2*], Eddy Jirón-García[3], Alfredo López[4], Fabian Villalta-Romero[5,6], Maria E. Ramírez-Ortiz[7]

[1] Centro de Investigación en Ciencias e Ingeniería de Materiales, Universidad de Costa Rica, San Pedro, 11501-2060 San José, Costa Rica
[2] Instituto de Investigaciones en Ingeniería, Universidad de Costa Rica, San Pedro, 11501-2060 San José, Costa Rica
[3] Universidad de Costa Rica, Sede del Caribe, Limón, Costa Rica
[4] Escuela de Ingeniería Química, Universidad de Costa Rica, San Pedro, 11501-2060 San José, Costa Rica
[5] Centro de Investigación en Biotecnología, Instituto Tecnológico Costarricense, Cartago, Costa Rica
[6] Escuela de Química, Instituto Tecnológico Costarricense, Cartago, Costa Rica
[7] Departamento de Ingeniería y Tecnología, Facultad de Estudios Superiores Cuautitlán, Universidad Nacional Autónoma de México, México
* Corresponding author's e-mail: karina.rodriguezmora@ucr.ac.cr

ABSTRACT

The development of microalgae-based agricultural biostimulants requires integrated production strategies that ensure biomass availability, formulation stability, and process scalability. This study developed and evaluated a pilot-scale production system integrating *Scenedesmus* sp. cultivation in a raceway reactor with the formulation and characterization of nanobentonite-stabilized oil-in-water Pickering emulsions. Microalgal biomass production was simulated using a MATLAB-based model and compared with experimental and published raceway data, showing good agreement. Emulsion processing conditions were investigated through experimental designs evaluating agitation speed, mixing time, and draft tube configuration. Among five oils evaluated, corn oil provided the longest microalgal viability half-life (145 days). A stable Pickering emulsion was obtained using 4 wt% nanobentonite and a 50:50 oil-to-water ratio. Fluorescence microscopy revealed microalgal cells dispersed in the aqueous phase and associated with oil droplets. Operating conditions of 2000 rpm and 10 min were selected for scale-up, while statistical analysis identified significant effects of mixing time, draft tube configuration, and their interaction on emulsion stability at extended processing times. Rheological characterization revealed yield-stress and shear-thinning behavior, adequately described by the Herschel–Bulkley model, indicating structural stability at rest and favorable flow properties during processing. Furthermore, the emulsion enhanced biostimulant performance compared with microalgae applied at an equivalent dose in water, increasing the germination index by approximately 200% relative to the positive control. Overall, these findings highlight the potential of integrating microalgal cultivation, formulation development, and process optimization to produce stable and effective agricultural biostimulants with potential for scale-up.

Keywords: sustainable agriculture, process design, biostimulant, circular bioeconomy, ecological enginerering.

INTRODUCTION

The extensive use of chemical fertilizers has played a key role in increasing agricultural productivity; however, their excessive application has led to significant environmental and soil degradation, including nutrient imbalances, soil compaction and salinization, and contamination of surface and groundwater by nitrates and phosphates. These impacts negatively affect soil

biodiversity and long-term fertility, limiting the sustainable development of modern agriculture. In response, biofertilizers have gained increasing attention as environmentally friendly alternatives capable of reducing dependence on synthetic inputs while supporting soil health and ecosystem stability (EL Mernissi and EL Arroussi, 2024; Gonçalves et al., 2023).

Soil degradation in Costa Rica is a major environmental and agricultural challenge driven mainly by water erosion in steep, high-rainfall regions, historically affecting over 40% of national soils and causing substantial losses of organic carbon, nutrients, and water-holding capacity, with economic impacts estimated at 7.7% of the agricultural gross product in past decades. In lowland intensive systems, particularly pineapple plantations in the Huetar Norte region, degradation is expressed through chemical and biological changes, including increased acidity, altered nutrient dynamics, and reduced soil biotic complexity, as indicated by nematode-based assessments. Overall, erosion, fertility decline, and deterioration of soil structure and biological activity reduce the sustainability of agricultural systems and increase dependence on external inputs (Cerretelli et al., 2023; IFPRI, 2026; Varela-Benavides et al., 2022).

Microalgae have emerged as promising biostimulants in agriculture due to their rich composition of bioactive compounds, including antioxidants, osmoprotectants, phytohormones, and proteins. These compounds enhance plant resilience to abiotic stresses such as drought, salinity, and heat, which are exacerbated by climate change. For instance, microalgal treatments have been shown to improve water-use efficiency, nutrient uptake, and photosynthetic activity in drought-stressed plants, leading to increased biomass and yield (Kusvuran and Kusvuran, 2019; S. Kusvuran, 2021). Under salt stress, microalgae can regulate ionic balance by reducing sodium uptake and increasing potassium levels, thereby mitigating ionic stress and improving plant growth and yield (A. Kusvuran and Can, 2020). Additionally, microalgae contribute to soil health and CO_2 sequestration, making them a sustainable option for modern agriculture (Safi et al., 2014; Sun et al., 2022).

As biostimulant, microalgae are a particularly promising resource due to their high nutritional value and multifaceted ecological roles. Microalgae are rich in amino acids, vitamins, minerals, and bioactive metabolites such as phytohormones, and many species can fix atmospheric nitrogen, contributing directly to plant nutrition. The incorporation of microalgal biomass into soils enhances organic matter content and nutrient availability and improves soil structure through the secretion of exopolysaccharides and other extracellular compounds that promote aggregate formation and stability. These processes increase soil porosity, water retention, aeration, and microbial activity, thereby supporting plant growth, maintaining soil fertility, and contributing to sustainable and ecologically engineered agricultural systems. Despite these benefits, further research is needed to explore their full potential, particularly in addressing heat stress and understanding the molecular mechanisms underlying their bio-stimulant effects (El Mernissi and EL Arroussi, 2024; Ronga et al., 2019; Song et al., 2024; Vangenechten et al., 2025).

One challenge is the stabilization and formulation of microalgae bio inputs. An interesting approach to formulation is the Pickering emulsions, formed by the irreversible adsorption of solid particles at the oil–water interface. They have emerged as a robust and environmentally friendly alternative to conventional surfactant-stabilized systems. The high desorption energy of colloidal particles confers exceptional stability to these emulsions, while enabling their formulation using biocompatible, low-toxicity and recyclable materials. In recent years, stimuli-responsive Pickering emulsions stabilized by nanoparticles have attracted increasing attention due to their functional versatility and reduced environmental impact. These characteristics position Pickering emulsions as a promising platform for ecological engineering applications, where interfacial design, material sustainability and process efficiency are critical, fostering multidisciplinary research and facilitating their translation into sustainable industrial and environmental technologies (Ge et al., 2022; Sun et al., 2022).

The production of microalgae-based biostimulants requires cultivation systems capable of supplying sufficient biomass for subsequent formulation. Open raceway ponds are suitable for this purpose; however, their scale-up presents challenges related to process control, biomass productivity, and resource utilization (Calijuri et al., 2022). In this context, the development of Pickering emulsions incorporating living microalgae, rather than conventional microalgal extracts or inactive biomass, represents an alternative approach to biostimulant formulation. Integrating

this formulation into a production process requires evaluating the compatibility between microalgal cultivation and emulsion preparation under suitable operating conditions. Therefore, this study proposes and evaluates an integrated production system that combines microalgal cultivation in a raceway reactor with the formulation of clay-stabilized Pickering emulsions containing living microalgae. Experimental results and process simulation were used to assess the technical feasibility of integrating both stages and scaling up the proposed system to pilot-scale production.

METHODOLOGY

Simulation and verification of microalgal production in a raceway system

Raceway cultivation was simulated using the software platform developed by the University of Almería (González-Hernández et al., 2024). The simulator was selected because it incorporates a dedicated raceway pond simulation module and integrates global climatic and environmental datasets to estimate microalgal productivity under site-specific conditions. This enables a preliminary assessment of cultivation feasibility before performing the detailed raceway simulation. In addition, the software has been developed and maintained by a research group with extensive experience in microalgal cultivation modeling, providing confidence in its scientific basis and long-term support.

For this study, the simulator was configured to represent the proposed pilot-scale system by setting the raceway cultivation area to 10 m^2, the culture depth to 0.15 m, and the initial biomass concentration to 0.5 $g \cdot L^{-1}$.

In parallel, the mass balance equations were implemented in MATLAB R2026a to estimate biomass production and the associated process streams. The biomass production predicted by the University of Almería simulator was subsequently compared with the values obtained from the MATLAB R2026a implementation. This comparison served as a verification step to verify the consistency of the independently developed model and to confirm that both approaches produced comparable biomass production estimates under the selected operating conditions.

The MATLAB model was calibrated against experimental data and subsequently used for process design and simulation. Figure 1 shows the raceway cultivation system used in the study.

Formulation system

Microalga cultivation

The microalgae used in this research were obtained from Centro de Investigación en Biotecnología, Instituto Tecnologico de Costa Rica. The culture was carried out under environmental conditions in Cartago, Costa Rica, in a 1 m^3 small tank with continuous air bubbling. In the exponential growth phase, biomass was harvested by centrifugation (Thermo Scientific, Sorvall

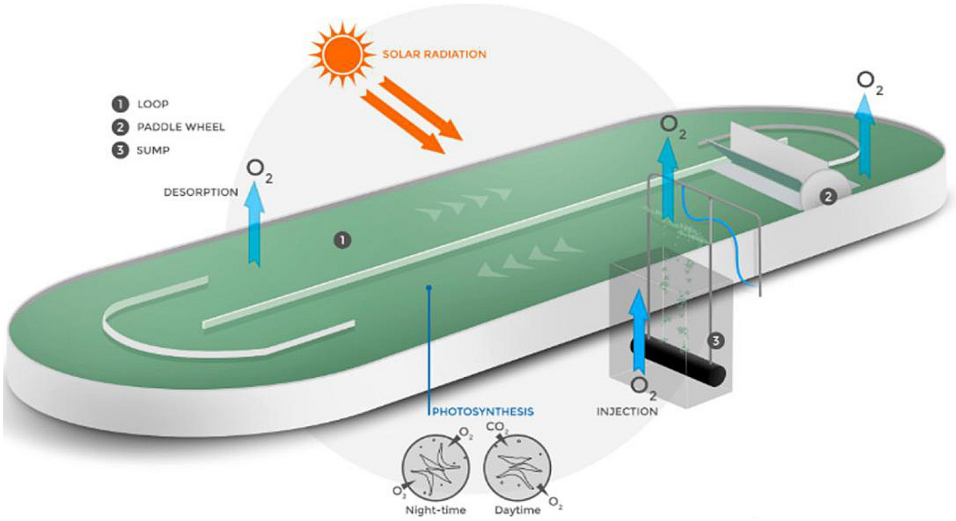

Figure 1. Raceway pond schematic. Source: RacewaySim Virtual Lab. Image generated with the tool developed by (Guzmán et al., 2025)

Legend X1R, USA) at 1000 × rpm for 10 min at 4 °C, then recovered and washed with sterile distilled water. The culturing medium was a mixture of Urea (0.63 g/L), potassium nitrate (0.085 g/L), and potassium dihydrogen phosphate (0.192 g/L). In the exponential growth phase, 15 days after the culture began, the culture density was 6 × 10^6 cells/mL. The biomass was harvested by centrifugation (Thermo Scientific, Sorvall Legend X1R, USA) at 710 × g at 4 °C for 10 min, then recovered and washed with sterile distilled water. (Covell et al., 2020; Villalta-romero et al., 2019)

Viability of microalgae in oils

Microalgal wet biomass was mixed with different commercial oils (canola, corn, sunflower, soybean, and paraffin oil) at a final biomass concentration of 5% (dry weight basis). All formulations were prepared at the beginning of the experiment and stored under the same conditions. Microalgal viability was evaluated monthly using three independent, previously unopened samples (n = 3) per formulation at each sampling time, ensuring that different experimental units were analyzed throughout the storage period.

For viability assessment, the samples were centrifuged (CENCE H1850) at 5000 rpm for 5 min, and the oil phase was removed by washing twice with distilled water, minimize potential interference, the microalgal biomass was resuspended in a volume of water equivalent to the initial volume of the oil phase.

Subsequently, 100 µL of the recovered microalgal suspension water (was mixed with 10 µL of fluorescein diacetate (FDA, 10 mg/L in acetone) and incubated for 15 min. Cell viability was assessed using fluorescence microscopy Zeiss Axio lab5, with a healthy microalgal culture serving as the positive control. Viability was monitored over time until it reached 50% or less of its initial value, allowing estimation of the viability half-life ($t_{1/2}$), defined as the time required for a 50% reduction in the initial viable cell population (Xiao et al., 2011).

Attenuated total reflection infrared spectroscopy of oils

ATR-FTIR (Perkin Elmer model Frontier) was used with a diamond base ATR and MCT/A detector, and 32 scans were performed from 4000 to 450 cm^{-1}. This experiment was carried out at the beginning and the end of the viability test. For these measurements, the microalgae were separated from the oils by centrifugation at 5000 rpm for 5 min (Wang et al., 2022).

Emulsion and stability

The emulsion formulation was based on the proportions previously reported by (Rodriguez-Mora et al, 2026b). However, modifications were introduced regarding the type of oil and the salt employed, following the recommendations of to improve microalgal viability.

The O/W emulsions were transferred to test tubes and placed at room temperature for different times. Then, the height of creamed emulsion phase in the test tube (*he*) and the height of the total fluid, which is the creamed emulsion phase + resolved water phase (*ht*), were measured. A stability factor (*Rh*) was used to characterize the emulsion stability against creaming. *Rh* was calculated from (*ht-he)/ht*. A greater *Rh* means a better emulsion stability against creaming.

The nanoclay was pulverized using a high-energy planetary micro mill (PULVERISETTE 7, Fritsch GmBH, Germany) as reported elsewhere (Arredondo-Tamayo et al., 2022; Hernández-Varela et al., 2021). A dry milling process was performed with agata balls (<5mm) for 30 min at a ratio of 1:72 (g material/nº balls), a grinding velocity of 800 rpm, and 5 min milling per 5 min pause. Pickering emulsions (O/W) were prepared by cross-linking technique according Wang and Alvarado, (2011) with some modifications. First KNO_3 were dissolved in water at 51 mM, then the nanoclay was dispersed at 3000rpm for 1 min, to obtain a final value of 4% w/v.

After that, corn oil with microalgae was added drop-by-drop and mixed for 2 min at 10000 rpm, using a high-speed homogenizer (T18 Ultra-turrax, IKA work Inc., USA. The finished emulsion was at 5g/L microalga in dry biomass. The samples were carried out in triplicate.

Emulsion characterization

The emulsion was examined using a Zeiss Axio Lab 5 fluorescence microscope to visualize the presence and distribution of microalgal cells within the Pickering emulsion. Bright-field microscopy was used to observe the emulsion structure, while chlorophyll autofluorescence was employed to identify microalgal cells. Fluorescence observations were performed using a 470 nm LED light source and a BP 469/38 excitation filte (Ou et al., 2007).

Biostimulant activity protocols

The selected dry biomass concentration was intended to produce a concentrated emulsion suitable for subsequent dilution in water at a ratio of 1:100 (v/v), yielding a final microbial concentration of 1×10^9 CFU mL^{-1}. This dilution ratio was selected to simulate a field application volume of 100 L ha^{-1}. Previous studies demonstrated that this microbial concentration provides the highest efficacy in biostimulant applications; therefore, it was adopted as the target concentration in this work (Rodríguez-Mora et al., 2026a). The biostimulant activity of the diluted Pickering emulsion was evaluated against both a positive control and a negative control consisting of water. All results were normalized relative to the negative control (water), which was assigned a value of 100%. Consequently, values exceeding 100% indicate a positive biostimulant effect compared with the water control.

Thickening of cotyledons

Commercial seeds of cucumber (*Cucumis sativus* L.) were used to evaluate the stimulant effect on germination (Navarro-López et al., 2020b). Cucumber seeds were placed in with 0.7% agar solidified KNOP nutrient medium that consists of 0.8 g/L of $Ca(NO_3)_2$, 0.2 g/L of KNO_3, 0.2 g/L of KH_2PO_4, 0.2 g/L of $Mg_2SO_4 \cdot 7\ H_2O$, and they were incubated at 25 °C in a dark chamber for 5 days. Once this time has passed, 3 mL of the treatment to be evaluated were added. Cotyledons were cut, separated, and were weighed, annotated, and transferred to Petri dishes. All this did it under green light or in darkness. Water was used as a negative control, and kinetine at 1 mg/L as a positive control; four replicates independent of each were made. The plates were incubated at 25 °C in the dark for 3 days. Cotyledons were dried on paper and weighed them again. The values were written down to calculate weight gained. Write down the values to calculate weight gain. (Morillas-España et al., 2022).

Germination rate

Germination was studied in commercial seed (Hayslip tomato seeds 493188-55). The experiments were carried out in triplicate, and for one of them, 25 seeds were used. Distilled water was used as a negative control, and gibberellic acid at 5 mg/L was used as a positive control. It was incubated in the dark at 25 °C for 3 days (Morillas-España et al., 2022). Each shoot's hypocotyl length was measured, and hypocotyl size was determined using ImageJ to compare seed germination rates across treatments with the controls.

$$GI(\%) = \frac{G \times L}{G_W \times L_W} \times 100 \quad (1)$$

where: G and L are the number of seeds germinated and the length of the hypocotyl of each treatment, while G_W and L_w correspond to the values obtained with water.

Root growth

Adventitious root growth is analyzed in stem cuttings. 2 cm of sterile perlite is added, moistened with water, and sorghum seeds are evenly placed on the perlite. Wait 10 days at 25 °C, with 65% humidity and fluorescent lamps. Once they are a uniform size, cut 3 cm below the cotyledon. Place 20 mL of each microalga in jars, with 2 cuttings in each vial, in triplicate. The leaves will be left out of the vial. Distilled water was used as a negative control, and IBA 3 mg/L as a control. The vials were placed again in light at 25 °C and 65% humidity for 4 days. After incubation, count the number of main roots of each cutting, larger than 1 mm, and compare each treatment with the controls (Morillas-España et al., 2022).

Tank design and scale-up criteria

Although the formulation composition had been previously standardized at laboratory scale using an Ultra-Turrax homogenizer, this equipment is not directly scalable to pilot-scale production. Therefore, an optimization stage was conducted to identify operating conditions capable of reproducing the emulsion stability achieved under laboratory conditions while enabling implementation in a stirred-tank system.

A laboratory-scale formulation tank (300 mL working volume) was designed and fabricated to perform the emulsion optimization experiments. The vessel was constructed from transparent acrylic to enable direct visualization of flow patterns, mixing behavior, and emulsion formation during operation. The agitation system was specifically developed for this study and consisted of a custom impeller designed using computer-aided design (CAD) software and manufactured by three-dimensional (3D) printing. The impeller was coupled to the drive shaft through a threaded

connection, providing mechanical stability while allowing rapid replacement or modification of the mixing element when required. The complete laboratory-scale formulation system is shown in Figure S1. The tank and impeller dimensions were established according to the geometric design criteria summarized in Tables S1 and S2, which served as the reference geometry for the subsequent scale-up procedure. A detailed representation of the agitation system, including the stirred tank configuration and impeller geometry, is presented in Figure 2.

A full factorial design (2^3) with two replicates was the first step conducted to determine the optimal operating conditions for the laboratory-scale emulsification tank. Experiments were performed using an IKA RW20 digital overhead stirrer. The investigation factors were agitation speed (600 and 2000 rpm), mixing time (5 and 10 min), and draft tube configuration (present or absent). The selected agitation speeds were chosen to evaluate the performance of the system under the high-torque (600 rpm) and low-torque (2000 rpm) operating regimes of the agitator. Emulsion stability at 1, 24, and 48 h was used as the response variable.

The analysis of the main effects and interactions showed that the operating conditions that maximized emulsion stability were identified. To further investigate the influence of mixing time, additional experiments were performed by extending the agitation period to 10, 20, and 30 min while maintaining a constant agitation speed to optimize the tank design. The experiments were conducted with and without a draft tube, and formulation stability was evaluated after 24 and 48 h. The effects of mixing time and draft tube configuration on formulation stability were analyzed separately for each storage period using a two-way analysis of variance (two-way ANOVA).

Based on the validated emulsion stability results, the agitation system was scaled up using a dynamic similarity approach by maintaining a constant power input per unit volume (P/V) between the laboratory-scale and pilot-scale systems. The pilot tank dimensions were determined by applying geometric similarity to the laboratory-scale vessel while maintaining the same height-to-tank diameter (H/T) ratio and the relative impeller diameter (D/T). Once the pilot tank geometry was established for the target working volume, the impeller rotational speed was calculated to satisfy the constant P/V criterion. The fluid viscosity used in the scale-up calculations was obtained from the rheological characterization of the emulsion and incorporated into the design procedure to ensure representative hydrodynamic conditions across both scales.

Rheological characterization of emulsion

The rheological characterization was conducted using emulsions prepared under the validated operating conditions identified in the previous optimization stage. The purpose of this characterization was to determine the rheological parameters necessary for process scale-up, including flow behavior and viscoelastic properties. These parameters served as input data for the design and simulation of the pilot-scale mixing system and for evaluating the hydrodynamic conditions required to maintain emulsion stability during production.

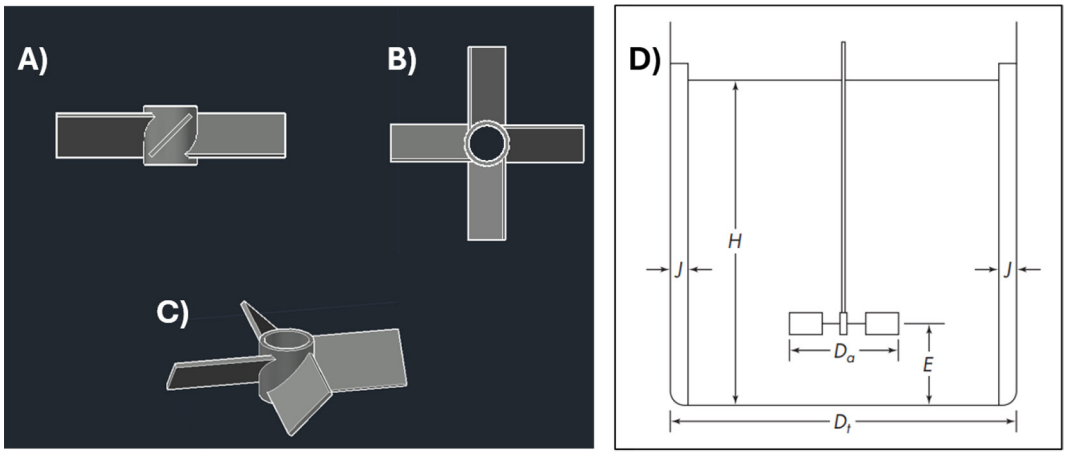

Figure 2. Geometry of the agitation system: (a) side view of the impeller, (b) top view of the impeller, (c) isometric view of the impeller, (d) stirred tank configuration showing the main design parameters

Rheological measurements were performed using a rotational rheometer (ARES-G2, TA Instruments) equipped with parallel plates (25 mm diameter, 1 mm gap) and operated with TRIOS software. All measurements were conducted at 25.0 ± 0.1 °C using a Peltier system. Flow curves were obtained under increasing and decreasing shear rates (1–500 s^{-1}) to determine flow behavior. The coefficient of variation (CV) between both curves was calculated to assess time dependency thixotropy (Wang and Alvarado, 2011).

Oscillatory tests were conducted to evaluate viscoelastic properties. An amplitude sweep (0.1–100% strain) at 1 Hz was first performed to determine the linear viscoelastic region (LVR). The LVR was defined as the range where storage modulus (G′) and loss modulus (G″) remained constant. The structural breakdown point was associated with the disruption of emulsion microstructure and loss of stability. A frequency sweep was subsequently carried out within the LVR, varying angular frequency (ω) from 0.1 to 100 rad·s^{-1}. Storage (G′) and loss (G″) moduli were recorded to characterize viscoelastic behavior. Apparent viscosity values derived from these measurements were used to adjust power consumption estimations. Three independent samples were prepared and analyzed for each experiment.

Biostimulant production process scale-up

Design considerations

The energy requirements and reagent consumption for the downstream formulation process were assumed to be proportional to those determined experimentally at laboratory scale. Specifically, the mixing tank and the rheological characterization of the emulsion were based on laboratory-scale experiments, whereas the annual microalgal biomass production was obtained from the raceway simulation. The nominal power of the system was estimated from the mechanical energy supplied by the raceway rotor, considering equipment efficiency. Energy consumption of the centrifuges, compressors, and the T-08 mixing tank rotor was calculated from nominal equipment specifications and manufacturer-reported efficiency factor. The physicochemical and biological properties of the microalgae and the structural and rheological characteristics of the emulsion were assumed to remain unchanged during scale-up and therefore equivalent to those measured at laboratory scale.

Raceway cultivation and biomass recovery

A pilot-scale raceway system was dimensioned and simulated based on the operational configuration of a representative microalgae production system. The design focused on key geometric parameters, including aspect ratio (length-to-width), culture depth, paddle wheel configuration, and channel curvature radius. The corresponding values are presented in Table S4. Hydrodynamic and operational parameters were determined, including flow velocity, hydraulic residence time (HRT), oxygen transfer, and power requirements for mixing. These parameters were used as input variables for system evaluation, relevant information is shown in Table S5. The raceway system simulation was implemented based on the framework described (Guzmán et al., 2025b), in which biomass concentration dynamics are described by the following growth kinetics:

$$\frac{dC_b(t)}{dt} = C_b(t)\left[\mu(t) - \frac{Q_d(t) - g_s(t)}{V(t)}\right] \quad (2)$$

where: $C_b(t)$ is the biomass concentration (kg·m^{-3}), $\mu(t)$ is the specific growth rate (d^{-1}), $Q_d(t)$ is the dilution flow rate ($m^3 \cdot d^{-1}$), $g_s(t)$ is the evaporation rate ($m^3 \cdot d^{-1}$), and $V(t)$ is the total culture volume (m^3). Values were showed in Table S6.

The system was operated at a constant temperature of 30 °C. The dissolved oxygen setpoint was fixed at 150% saturation, with a maximum air flow rate of 100 L·min^{-1}. The pH was controlled at 8.0 using a proportional–integral (PI) controller with a proportional gain of −0.001 and an integral constant of 2000. The values are shown at Table S7. In the biological submodel, a light extinction coefficient of 0.05 $m^2 \cdot g^{-1}$, a light saturation intensity of 130 W·m^{-2}, and a shape parameter of 2 were used. The thermal growth range was defined as 5/30/40 °C (minimum/optimal/maximum), while the pH growth range was set to 6.5/8.0/9.0.

The simulation was configured using representative geographic coordinates and climatic conditions for Costa Rica (longitude −84.014°, latitude 10.217°, altitude 151 m above sea level), which were employed by the simulation platform as a reference location for the country. October 15, 2025, selected as the reference date. The dynamic mass balances for dissolved oxygen (DO) and total inorganic carbon (TIC) were based on the

model described by Fernández et al. (2016). The dissolved oxygen balance can be expressed as:

$$\frac{d(DO \cdot V)}{dt} = R_{O_2,\text{photo}} - k_L a^{O_2}(DO - DO^*)V - \\ - Q_h\, DO + Q_d\, DO_{in} + R_{air} \quad (3)$$

where: $R_{O_2,\text{photo}}$ is the oxygen production rate due to photosynthesis, DO^* is the equilibrium (saturation) concentration with the gas phase, and $k_L a^{O_2}$ is the volumetric mass transfer coefficient for oxygen.

If explicitly considered, R_{air} represents the contribution of the aeration system to oxygen transfer.

$$\frac{d(TIC \cdot V)}{dt} = -R_{C,\text{photo}} - k_L a^{CO_2}(CO_2 - CO_2^*)V - \\ - Q_h\, TIC + Q_d\, TIC_{in} + R_{CO_2} \quad (4)$$

where: $R_{C,\text{photo}}$ represents the photosynthetic carbon uptake rate, CO_2^* is the equilibrium concentration with the gas phase, and R_{CO_2} accounts for the addition of CO_2 associated with pH control.

The raceway system, including paddlewheel configuration and head losses, was dimensioned according to the parameters presented in Tables S8–S10. Culture medium was prepared by adding urea (0.63 g·L^{-1}), potassium nitrate (0.085 g·L^{-1}), and potassium dihydrogen phosphate (0.192 g·L^{-1}) (Villalta-Romero et al., 2019) to a total working volume of 1.5 m³.

The system was inoculated with 0.5 g·L^{-1} of microalgae to reach the final concentration predicted by simulation. Mixing was achieved using a paddlewheel (60 cm blade length), generating a flow velocity of 0.2 m·s^{-1}. Aeration was supplied at 100 L·min^{-1}, with a PID controller setpoint defined in the simulator (integration constant: 2000 s^{-1}; proportional constant: −0.001).

Harvesting was performed every 48 h, removing 20% of total volume until pseudo-steady-state conditions were reached. The harvested stream was directed to a buffer tank and subsequently subjected to centrifugation at 9000 rpm for 10 min, yielding biomass with approximately 83% moisture content.

RESULTS AND DISCUSSION

Simulation and verification of microalgal production in a raceway system

Computational tools play a critical role in the predictive assessment of microalgae production systems. In this context, the graphical tool developed by the University of Almería enables the estimation of microalgal productivity in raceway reactors across different geographical regions, based primarily on meteorological inputs such as solar radiation and temperature (González-Hernández et al., 2024). Microalgae are photosynthetic organisms whose growth is influenced by multiple factors, including light intensity, temperature, pH, dissolved oxygen, and nutrient availability (Sánchez-zurano et al., 2021). However, within this simulation framework, process variables are assumed to be controlled, and productivity variations are mainly attributed to climatic conditions.

Figure 3A presents the global simulation results, indicating that Central America exhibits among the highest potential productivities, which is consistent with its proximity to the equator and the associated high solar irradiance throughout the year. Figure 3B shows the temporal variation in biomass production for Costa Rica, where productivity is not constant and fluctuates according to changes in radiation and temperature. Nevertheless, the country remains within a highly favorable production zone.

According to the model, the estimated annual biomass production is 610.5 kg of dry weight, corresponding to an average productivity of approximately 1.67 kg·day^{-1} for the evaluated system. In comparison, the MatLab model indicated 606.26 kg of dry weight annual, corresponding to an average productivity of 1.66 kg·day^{-1}.

The close agreement between the annual biomass production predicted by the University of Almería simulator and the independently developed MATLAB model confirms the consistency of both approaches for estimating microalgal productivity under the evaluated operating conditions. Based on these results, the MATLAB model was adopted for the subsequent scale-up analysis, as it enables direct integration of the culture medium formulation developed by the Tecnológico de Costa Rica (TEC) and provides detailed estimates of nutrient consumption throughout the cultivation process. This implementation also ensures

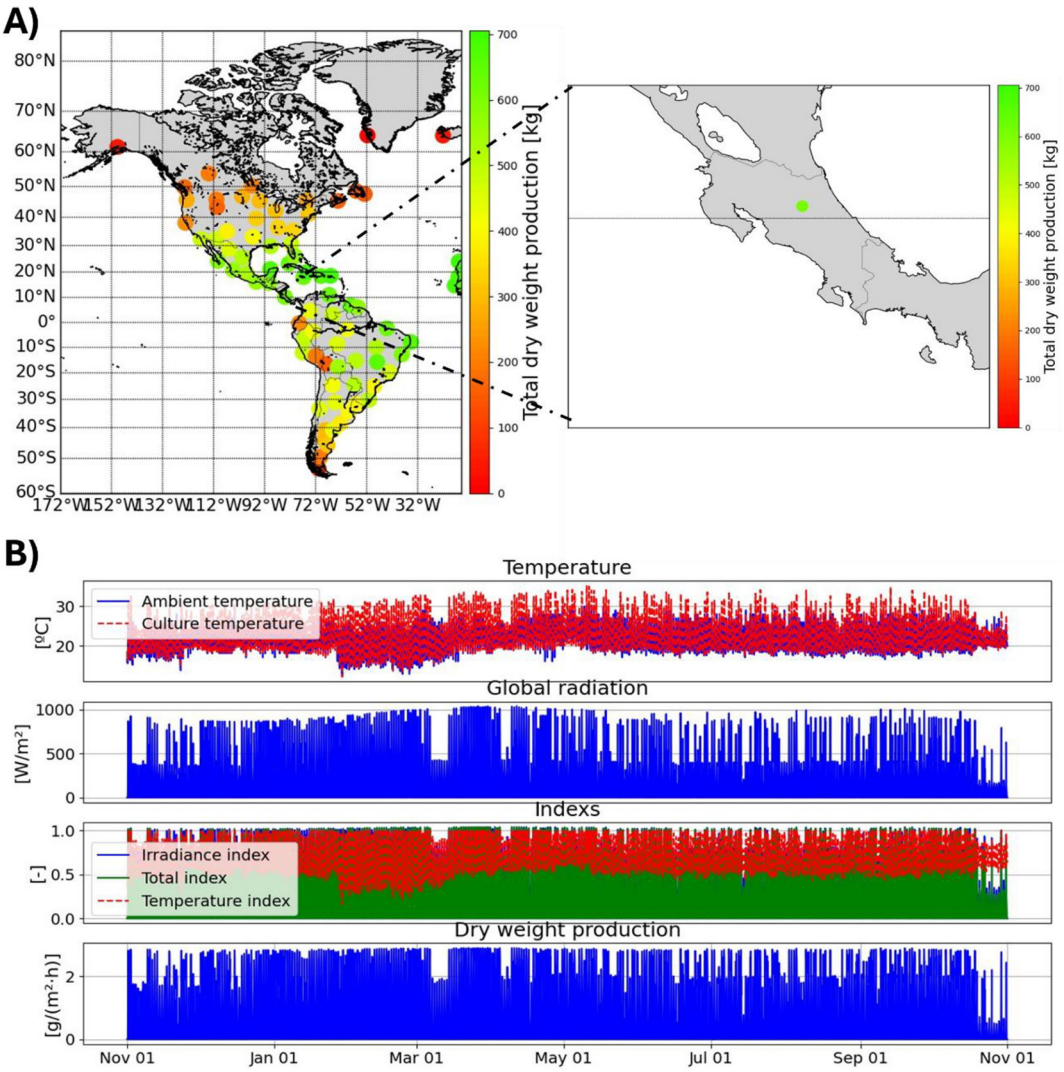

Figure 3. Simulation of *Scenedesmus* sp. production in a 10 m² reactor at a depth of 0.15 m, where (A) represents the annual production potential across the America and the annual production for Costa Rica. (B) Temporal variation in microalgal biomass production under Costa Rican climatic conditions. Image generated with the tool developed by (González-Hernández et al., 2024)

improved mass balance closure and traceability of biomass production, allowing a more accurate determination of raw material requirements and process streams for the pilot-scale biostimulant production system.

Formulation system

Agricultural bio-inputs derived from microalgae require preservation methods that maintain viability and minimize compositional changes. These methods typically involve reducing moisture or oxygen levels, as both factors contribute to greater microbial stability. Depending on the operational conditions, preservation can be achieved for either short- or long-term storage. Among the most employed short-term strategies are pH reduction and the establishment of anaerobic conditions. The latter promotes the formation of fermentation products, such as lactic acid, which in turn stabilizes the biomass. (Wendt et al., 2019)

In this case, short-term preservation was evaluated using different oils, as they can act as barriers to gas exchange, whether CO_2 for photosynthesis or O_2 for nocturnal respiration. Our objective was not to maintain the compositional balance as in strain-type storage, commonly employed for fungi and bacteria to preserve microorganisms in a semi-dormant state, conserving not only viability but also morphological characteristics.(Surja et al., 2020; Tamara and Slanina, 2022) Rather, a half-life that provides sufficient

field application capacity to ensure the effectiveness of the final product.

Figure 4 shows the viability study of *Scenedesmus* sp. with respect to the different oils used. In this case, oils such as paraffin and soybean were measured only once because their viability was below 50%, a threshold established to ensure an adequate shelf life for the final product. In contrast, corn oil exhibited the longest viability period, reaching 145 days, corresponding to an approximate application window of 5 months.

Qualitative changes in the different oils were analyzed during the half-life period determined in Figure 5. None of the studies revealed significant alterations in oil composition, whether due to degradation or the release of compounds into the medium during the evaluation period. All signals corresponded to characteristic bands of the oils. Table 1 presents the bands for corn, canola, soybean, and sunflower oils, while Table 2 shows the characteristic bands of paraffin oil. As a petroleum-derived product, paraffin oil predominantly exhibits structures of saturated hydrocarbons, both linear and branched, ranging from C15 to C50. In contrast, vegetable oils are derived from fatty acids and exhibit varying degrees of unsaturation and ester linkages (Sota-Uba et al., 2021; Wang et al., 2022).

Subsequently, corn oil was selected as the oily phase for emulsion preparation based on the microalgal viability results shown in Figure 1, where the microalgae remained well dispersed within the oil phase. The zeta potential (ζ) of the nanobentonite was −37.8 ± 4.9 mV, indicating adequate colloidal stability in the aqueous medium. To moderately reduce |ζ| and promote particle approach and interfacial adsorption, KNO_3 (51 mM) was dissolved in the aqueous phase. This adjustment facilitated particle packing at the oil–water

Table 1. Assignment of characteristic infrared absorption bands in corn, sunflower, canola, and soybean oils

Wavenumber (cm^{-1})	Assignment
3009	=C-H (cis) stretching
2922	CH_2 stretching (symmetric)
2853	CH_2 stretching (asymmetric)
1743	-C=O stretching of the ester group
1465	-C-H bending (asymmetric) of CH_2 o CH_3
1378	=C–H bending
1226	-C-O stretching o -C-H_2 bending
1160	-C-O stretching
1087	-C-O stretching
711	-HC=CH- (cis) o CH_2

Table 2. Assignment of characteristic infrared absorption bands in paraffin oil

Wavenumber (cm^{-1})	Assignment
2930	CH_2 stretching (symmetric)
2861	CH_2 stretching (asymmetric)
1454	–CH_2– (scissoring)
1365	–CH_3 (bending)
730	–(CH_2)n Rocking

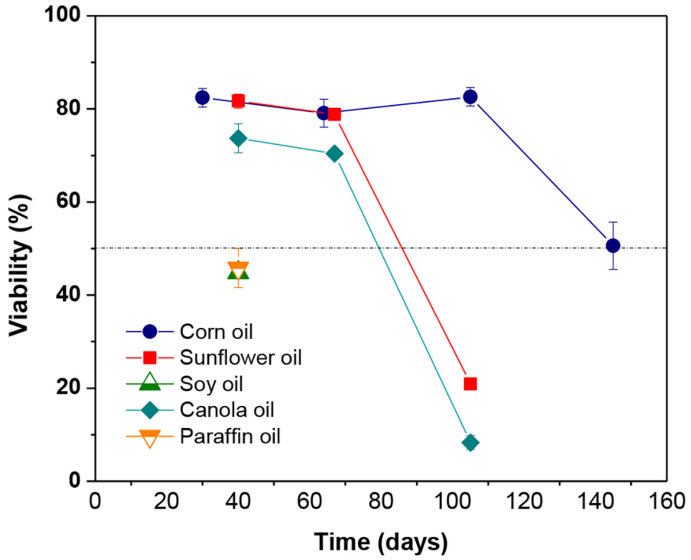

Figure 4. Viability study of *Scenedesmus* sp. in different oils

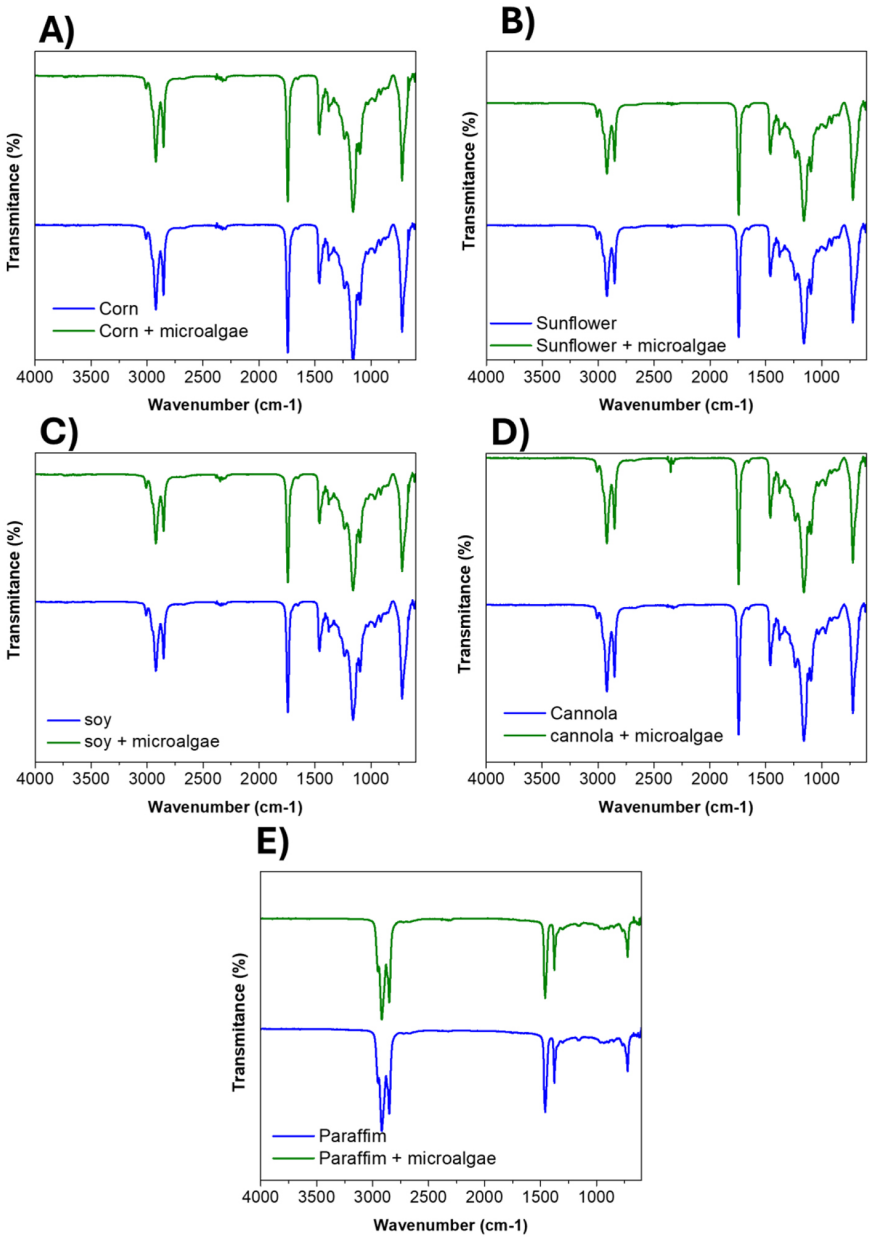

Figure 5. FTIR spectra of the different preservation oils before and after half-life evaluation with *Scenedesmus* sp.

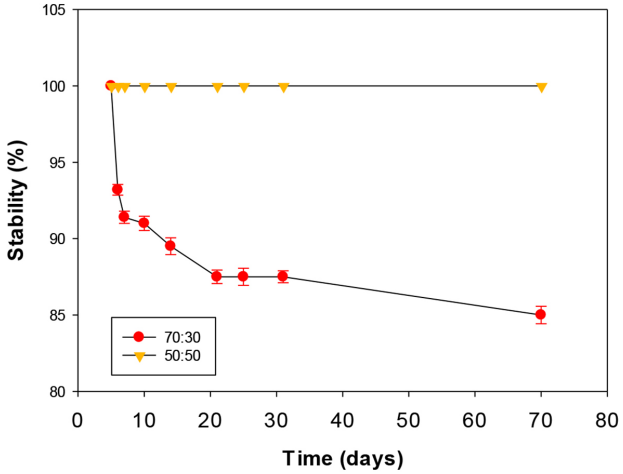

Figure 6. Emulsion stability of nanobentonite-stabilized oil-in-water (O/W) systems at different oil-to-water ratios over time

interface, leading to the formation of smaller droplets and a more continuous interfacial layer. Oil-in-water emulsions were prepared at two oil-to-water ratios (50:50 and 70:30), using a fixed nanobentonite concentration of 4 wt%.

Figure 6 shows the stability of both emulsion ratios. The most stable emulsion over the 70-day study period was the 50:50 oil-in-water (O/W) formulation, which was therefore selected for the microalgae (*Scenedesmus* sp.) encapsulation process. It is worth noting that both emulsions exhibited high stability; however, the 70:30 ratio showed sedimentation.

To identify the encapsulation process, fluorescence microscopy was performed. Microalgae exhibit autofluorescence due to the presence of chlorophyll, which emits red light upon excitation (Figure 8A). In contrast, the emulsion control appears blue (Figure 8B) due to light scattering. This effect occurs because the light source

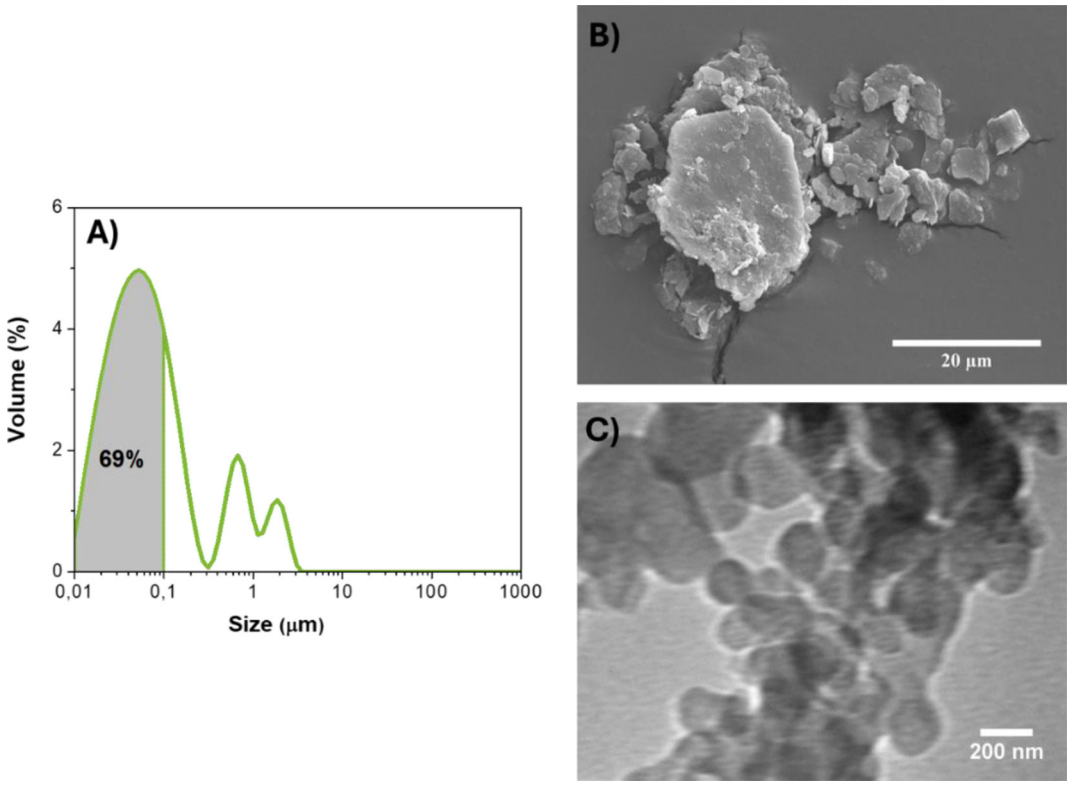

Figure 7. (A) Particle size distribution after milling, (B) SEM micrographs before milling, (C) TEM micrographs after milling

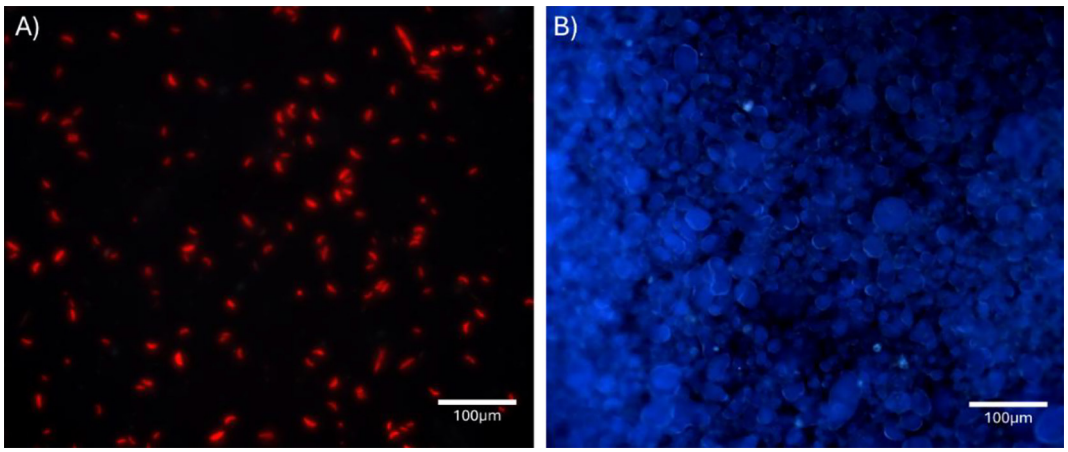

Figure 8. Fluorescence microscopy images of the control samples: (A) microalgae and (B) emulsion stabilized with nanobentonite

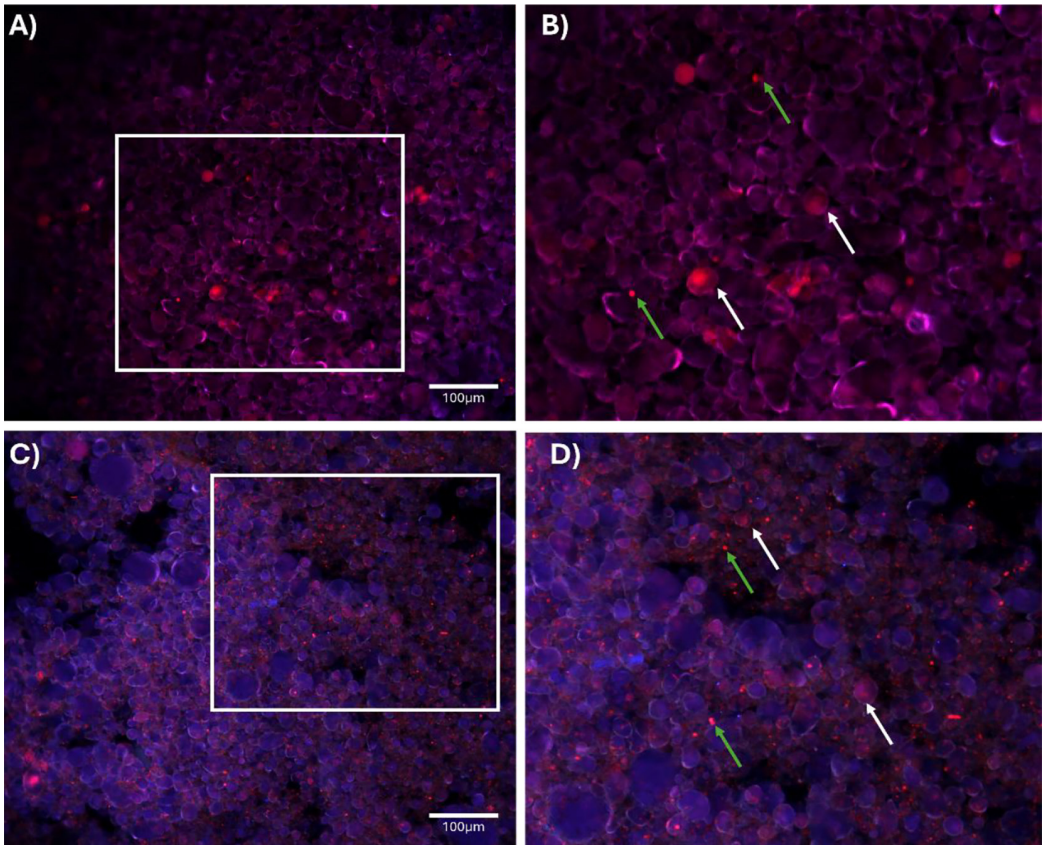

Figure 9. Fluorescence microscopy images of the nanobentonite-stabilized emulsion containing microalgae: (A, C) different sections of the emulsion, (B, D) magnified views of the corresponding areas. Green arrows indicate examples of free microalgae, whereas white arrows indicate encapsulated microalgae

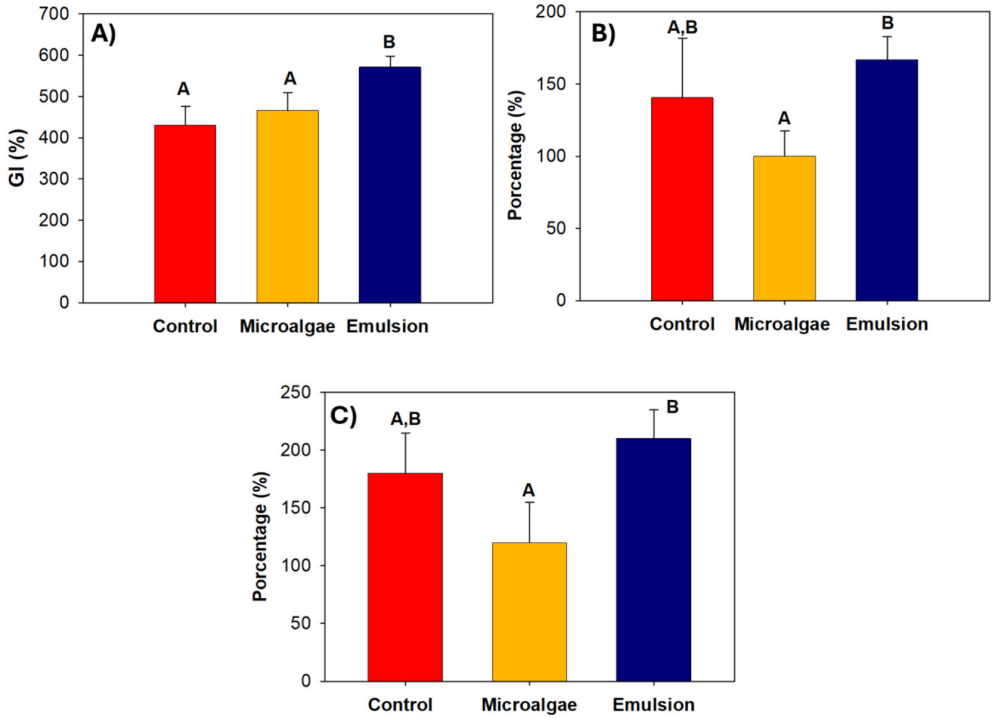

Figure 10. Bioassay results evaluating plant physiological responses: (A) seed germination using gibberellic acid (5 mg L^{-1}) as control (B) cotyledon thickening induced by kinetine (1 mg L^{-1}); and (C) root growth promoted by indole-3-butyric acid (IBA, 3 mg L^{-1}). The microalgae and the emulsion used dose 1.0×10^6 cells/mL. Different letters indicate significant differences ($p < 0.05$) within each treatment

is not monochromatic and the clay particles are predominantly nanoscale. As shown in Figure 7, colloidal particles scatter light because their size is comparable to the wavelength, making the scattering intensity proportional to particle size and refractive index contrast (Berne and Pecora, 2000; Murphy, 1997).

Figures 9A and 9C show different sections of the emulsion, while Figures 9B and 9D present magnified views of the previous images. Green arrows indicate microalgae that remain free in the aqueous or continuous phase, whereas white arrows highlight some microalgae encapsulated within oil droplets. Free microalgae appear as points of high intensity, whereas encapsulated ones appear diffused and exhibit purple hues within the droplets, resulting from the combination of red and blue fluorescence.

The results obtained from the different protocols were expressed as percentages relative to the negative control (distilled water), while a positive control was included in each experimental set for comparison. Overall, the treatments exhibited a marked enhancement in biological response, with the germination index reaching values of approximately 200% (Figure 10A) relative to the positive control. Auxins are widely recognized for their role in promoting root initiation and elongation. Among plant growth regulators, kinetin has been reported to enhance cotyledon thickening (Vildanova et al., 2023). As shown in Figure 10B and 10C, the evaluated treatment achieved a response comparable to the positive control, while exhibiting a greater effect than treatments based solely on microalgae.

The observed responses are higher than those previously reported in the literature (Navarro-López et al., 2020). However, it is important to note that those studies employed hydrolysates at concentrations expressed in g L^{-1}, whereas the present study utilizes live microalgae rather than extracted fractions. This distinction is critical, as it implies a different mode of action and bioavailability of active compounds. It is also important to emphasize that, when using live microalgae, the observed effects cannot be exclusively attributed to phytohormones. Microalgae are rich in amino acids, vitamins, minerals, and a wide range of bioactive metabolites, including phytohormones, which at excessive concentrations may even exert inhibitory effects rather than stimulation. (Ferreira et al., 2024) Therefore, the mechanism of action is inherently more complex and likely involves synergistic interactions among multiple biochemical constituents.

Across all evaluated protocols, the use of the Pickering emulsion resulted in reduced data dispersion, indicating improved experimental reproducibility. This suggests that the encapsulation matrix contributes to a more controlled and homogeneous delivery of bioactive components.

The Pareto analysis revealed that the relative importance of the process variables changed with storage time. At 1 h, Figure S2, agitation speed and the presence of a draft tube exhibited the strongest statistically significant effects on emulsion stability, while mixing time and several interaction terms also exceeded the significance threshold. These results indicate that the hydrodynamic conditions established during emulsification strongly influence the initial emulsion structure. After 24 h of storage, Figure S3, the influence of the draft tube decreased substantially and only agitation speed remained statistically significant, whereas mixing time was close to the significance threshold. This behavior suggests that the short-term benefits associated with flow pattern modification become less important as the emulsion evolves during storage.

At 48 h, Figure 11, agitation speed and mixing time were the dominant significant factors, whereas the draft tube no longer exerted a relevant effect. The increasing importance of these variables over time indicates that long-term emulsion stability is primarily governed by the total energy input delivered during emulsification rather than by the specific flow configuration inside the vessel. Therefore, the operating conditions selected for scale-up correspond to an agitation speed of 2000 rpm and a mixing time of 10 min**.** Interaction plots derived from the factorial analysis of the emulsion formulation conditions of storage are presented in Figures S5–S9.

To further evaluate whether extending the mixing time beyond the conditions identified in the factorial design could optimize formulation stability, additional experiments were conducted at the selected agitation speed (2000 rpm) using mixing times of 10, 20, and 30 min, with and without a draft tube. Prior to the statistical analysis, validation experiments were conducted to verify the reproducibility of the optimized formulation procedure. No statistically significant differences were observed between the original and validation experiments for either the draft tube or no-draft-tube configurations after 24 h

(p = 0.532 and p = 0.132, respectively) or after 48 h (p = 0.632 and p = 0.064, respectively), confirming the reproducibility of the experimental methodology. Subsequently, a two-way analysis of variance (two-way ANOVA) was performed to evaluate the effects of mixing time and draft tube configuration on formulation stability. Both mixing time and draft tube configuration significantly affected formulation stability after 24 h (mixing time: $p = 1.79 \times 10^{-5}$; draft tube: $p = 4.75 \times 10^{-8}$) and after 48 h (mixing time: $p = 3.37 \times 10^{-5}$; draft tube: $p = 1.99 \times 10^{-7}$). A significant interaction between mixing time and draft tube configuration was also observed after both 24 h (p = 0.00121) and 48 h (p = 0.000991), indicating that the effect of mixing time depended on the hydrodynamic configuration of the mixing system. In the absence of a draft tube, formulation stability increased substantially as the mixing time was extended from 10 to 30 min, whereas only minor improvements were observed when a draft tube was incorporated. These findings indicate that the draft tube enhanced fluid circulation and mixing efficiency, allowing high emulsion stability to be achieved even at the shortest mixing time evaluated. Consequently, extending the agitation time beyond 10 min provided limited additional benefit in the presence of a draft tube but was essential for improving formulation stability when the draft tube was absent. Figure S10 and S11 and Tables S11 and S12.

Based on the factorial design and the subsequent validation experiments, the formulation exhibiting the highest stability (10 min with draft tube) was selected for further characterization. Rheological analyses were performed to determine the flow behavior of the optimized Pickering emulsion and to evaluate its suitability for pumping, handling, and scale-up operations.

After identifying the operating conditions that produced the highest formulation stability, the optimized Pickering emulsion was subjected to rheological characterization. This analysis provides the engineering parameters necessary to describe the flow behavior of the formulation and to support equipment design, process simulation, and scale-up. In addition, the rheological response offers valuable information on the structural integrity of the emulsion under different shear conditions (Zhai et al., 2023). The rheological behavior of the optimized formulation is presented in Figure 12 whereas the fitted model parameters are summarized in Table 3.

In general, at low shear rates (< 10 s^{-1}), the emulsion exhibits high viscosity and a near

Table 3. Parameters obtained from the Herschel–Bulkley model

Yield stress (Pa)	Viscosity (Pa·s)	Rate índex	R
T_0	k	n	–
9.75±0.49	0.24±0.02	0.76±0.04	0.9993±0.0002

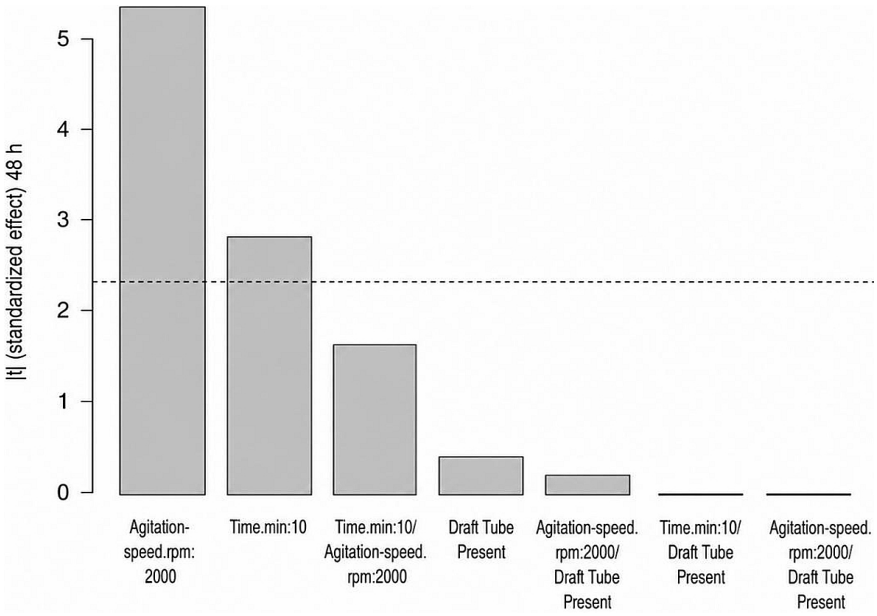

Figure 11. Pareto chart from the factorial analysis of emulsion formulation conditions after 48 h

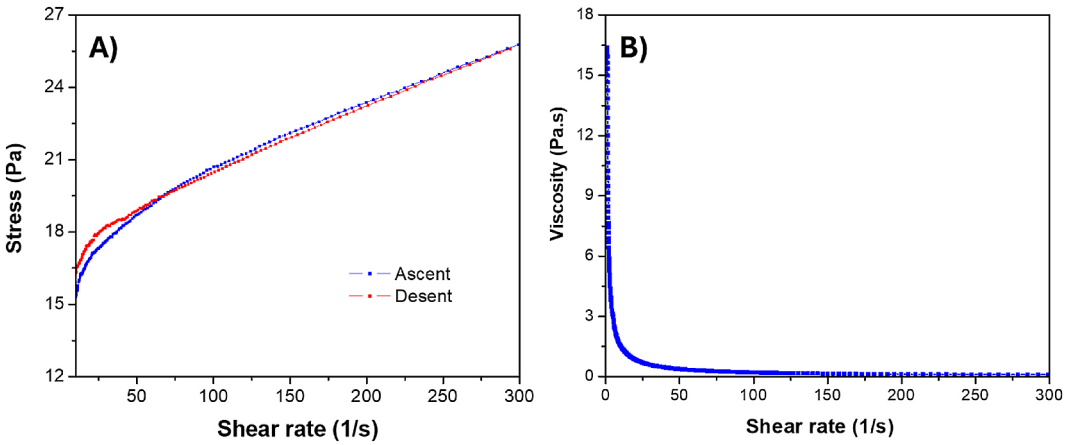

Figure 12. Rheological characterization of the emulsion: A) rheogram, B) flow curve

solid-like behavior, which reduces droplet mobility, thereby retarding coalescence and gravitational separation (Jeon and Hong, 2014). At higher shear rates (> 100 s^{-1}), the viscosity decreases markedly, facilitating mixing, pumping, and filling operations.

From a process and design perspective, the rheological parameters indicate that the clay-based Pickering emulsion exhibits a yield stress, shear-thinning behavior, well described by the Herschel–Bulkley model, recognized as the most suitable model for describing the rheology of natural clays (Jeong et al., 2012).

The yield stress (τ_0 = 9.75 ± 0.49 Pa) suggests the presence of a structured internal network, attributed to the adsorption and organization of clay particles at the oil–water interface and within the continuous phase, which enhances resistance to phase separation phenomena such as creaming or sedimentation during storage. The consistency index (k = 0.24 ± 0.02 Pa·s^n) reflects a moderate viscosity level, ensuring structural integrity while maintaining manageable flow conditions during processing. The flow behavior index (n = 0.76 ± 0.04) confirms a pseudoplastic response, indicating a decrease in apparent viscosity with increasing shear rate, which is advantageous for unit operations such as mixing, pumping, and spraying. The high coefficient of determination (R^2 = 0.9993 ± 0.0002) demonstrates an excellent fit of the model, supporting its reliability for process simulation, scale-up, and equipment selection. Overall, the emulsion exhibits a suitable balance between stability at rest and processability under shear, which is critical for its implementation in practical applications.

From a design perspective, the system exhibits a structured viscoelastic behavior (G′ > G″) with a well-defined linear viscoelastic region (LVR), confirming the formation of a stable particle network that resists deformation under low stress. This is particularly relevant as it defines a safe operational window for storage and handling without structural breakdown. At higher stresses, the decrease in moduli—especially G′—indicates controlled structural disruption and transition

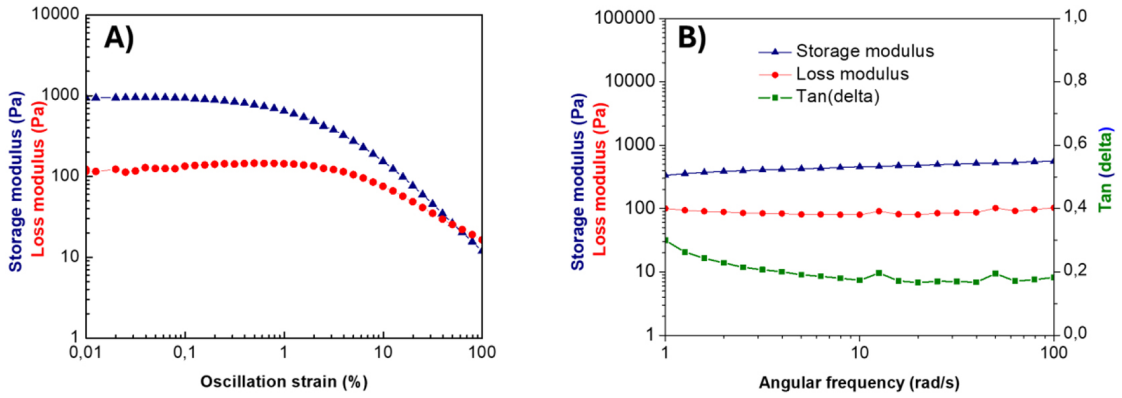

Figure 13. Oscillatory rheological behavior of pickering emulsion

to flow behavior, which is essential for unit operations such as pumping, mixing, and spraying (Figure 13A).

The figure confirms a predominantly elastic behavior ($G' > G''$) with low frequency dependence, indicating a stable and well-structured network. The low tan(δ) values (<1) reinforce structural dominance and resistance to phase separation. Such structural confinement limits droplet mobility, reducing the likelihood of coalescence, as observed in Figure 6B (Tadros, 2013). From a design perspective, this ensures stability during storage and robustness under process conditions, supporting scalable handling and application.

This formulation integrated high structural stability at rest with shear-induced fluidization, enabling both long-term stability and efficient processability, which is a key criterion for scalable design.

Biostimulant production process scale-up

The global simulation tool was used to estimate the productive potential of microalgae in Costa Rica based on climatic variables. Subsequently, RacewaySim enabled refinement of this estimation through an operational simulation of the raceway system, incorporating control variables such as pH, dissolved oxygen, harvesting, and dilution, in addition to geographical location and reactor geometry. The simulation is governed by a coupled biological growth and mass transfer model (Guzmán et al., 2025)

The biological model describes microalgal growth within the reactor, where biomass concentration is defined by Equation 5. In this expression, μ(t) represents the specific growth rate, the evaporation rate, the dilution flow rate, and the total reactor volume:

$$\frac{dC_b(t)}{dt} = C_b(t)\left(\mu(t) - \frac{Q_d(t) - g_s(t)}{V(t)}\right) \quad (5)$$

Model parameters were obtained from (Fernández et al., 2016). Additionally, dynamic mass balances for dissolved oxygen and total inorganic carbon were included, considering key phenomena such as gas transfer with the atmosphere, microalgal photosynthesis, reactor dilution, and air or CO_2 bubbling (Guzmán et al., 2025); (Fernández et al., 2016)

Simulation results indicate that the total biomass production within the bioreactor, under recalculated operational conditions, reaches 0.302 kg·day^{-1}. This value is in close agreement with the prediction obtained from the global simulation tool (0.3666 kg·day^{-1}). The slight difference can be attributed to the idealized assumptions of the global model, whereas RacewaySim incorporates more detailed operational parameters and dynamic system behavior.

Figure 14 shows that the reactor reaches a cyclic operating regime. Biomass concentration increases from 0.5 g·L^{-1} and, after approximately 300 h, begins to oscillate while maintaining sustained production, indicating that the average net growth rate exceeds the effective harvesting rate. Total inorganic carbon (TIC) exhibits an oscillatory profile with a gradual decline until stabilizing

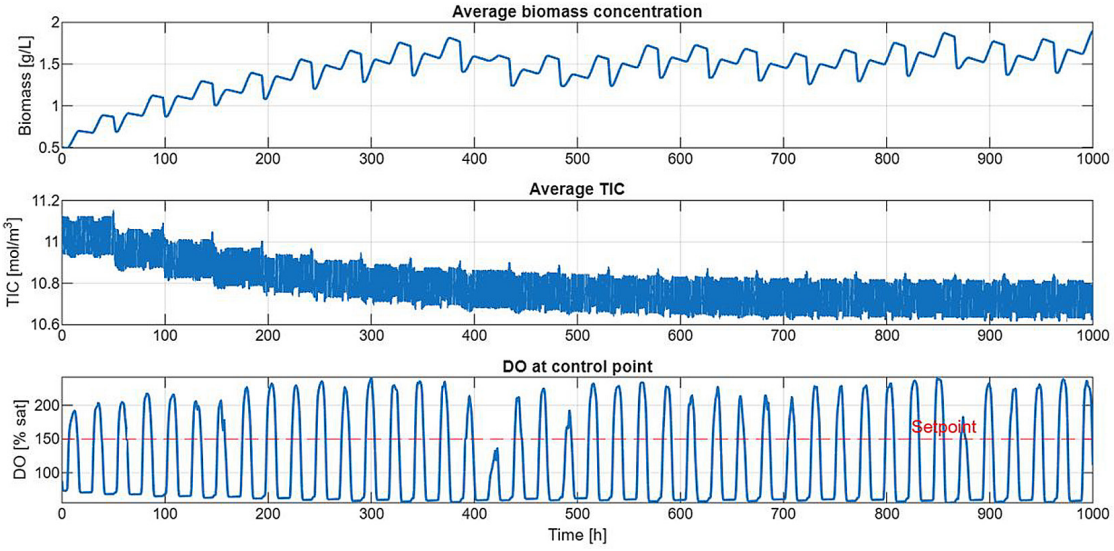

Figure 14. Representation of the microalgal growth conditions

within a relatively narrow band, suggesting continuous carbon consumption without depletion; therefore, the culture does not experience carbon limitation. In contrast, dissolved oxygen (DO) displays wide oscillations, ranging from 60% to over 200% of saturation. This behavior indicates that control strategy effectively prevents indefinite oxygen accumulation, albeit with a sharp response and noticeable overshoot, while still maintaining oxygen levels within productive ranges. Elevated DO concentrations, typically associated with intense (Gao et al., 2022)

In terms of productivity, the observed behavior is both promising and consistent with the requirements for microalgal biomass production under Costa Rican conditions, showing good agreement with the simulation frameworks reported in (Guzmán et al., 2025b). The discrepancy may be attributed to the photosynthetic growth rate assumed in the developed model (Costache et al., 2013). Similarly, differences may also arise from the parameterization of the equations in the model of (Fernández et al., 2016) as adapted for the raceway system. Given that the harvest concentration oscillates between 1.5–1.7 g·L^{-1}.

The proposed pilot plant, is designed to convert harvested microalgal biomass into a formulated product consisting of microalgae encapsulated within a Pickering emulsion. This formulation strategy offers advantages over conventional applications by enhancing the stability and viability of the microalgal biomass during storage and application (Qi et al., 2024).

To establish the operating conditions for the pilot-scale emulsification tank, the scale-up procedure was based on maintaining a constant energy input per unit volume (E/V) between the laboratory and pilot scales. The emulsion was initially prepared on a laboratory-scale, ideally stirred and baffled tank with a working volume of 300 mL. This configuration was chosen to establish the operating conditions required for subsequent scale-up to pilot scale while preserving the emulsion stability and mixing characteristics achieved at laboratory scale. This scale-up criterion was selected because emulsion stability was found to depend primarily on the energy supplied during mixing. The energy input per unit volume was calculated according to Equations 6 and 7, where the total energy transferred to the system is related to the power consumption, mixing time, and tank volume.

$$\frac{E}{V} = \frac{P}{V}\, t \tag{6}$$

$$\frac{E}{V} = N_p\, \rho\, N^3\, \frac{D^5}{V}\, t \tag{7}$$

In these equations, is the energy input per unit volume (J m^{-3}), is the power consumption (W), is the mixing time (s), is the power number, is the fluid density (kg m^{-3}), is the impeller rotational speed (s^{-1}), is the impeller diameter (m), and is the working volume of the tank (m^3). Based on these equations and the rheological characterization of the optimized Pickering emulsion, the operating conditions required for pilot-scale operation were determined. According to the rheological analysis, the emulsions exhibited low viscosity at high shear rates, indicating that the mixing process could be operated under turbulent flow conditions. Therefore, the power number was assumed constant during scale-up. Based on this criterion, supplying the same energy per unit volume in the 50 L pilot-scale tank requires an agitation speed of 2000 rpm for 98 min using a four-blade pitched turbine impeller at 45°. This tank capacity was selected to ensure consistency with the biomass production system while representing a realistic scale for pilot-scale implementation under local conditions. Furthermore, considering that approximately 1 L of formulated product is sufficient to treat 1 ha of agricultural land, the selected batch volume provides a practical basis for evaluating process performance and future scale-up scenarios.(Bernal-Samaniego, 2021).

Figure 15 and Table 4 summarize the scale-up process design based on a 50 L emulsion formulation tank and the corresponding raceway biomass production system, considering the average biomass productivity adopted for design purposes.

Based on the selected operating conditions, a single raceway harvest yields approximately 0.623 kg of dry biomass contained in 0.3 m^3 of culture broth. For the production of one 50 L batch of Pickering emulsion, only 0.128 m^3 of harvested broth is required, generating 1.47 kg of concentrated wet biomass after centrifugation, equivalent to 0.250 kg of dry biomass. This amount satisfies the target biomass concentration of 5 g L^{-1} in the final emulsion. The results indicate that the raceway production capacity is compatible with the downstream formulation unit, while the material requirements for water, oil, KNO_3, and bentonite remain within ranges suitable for pilot-scale operation.

Because no heat-exchange equipment is incorporated into the proposed pilot plant and changes in elevation and flow velocity are negligible, the process energy balance was simplified to the electrical and mechanical energy consumption associated with the operating units, in table S13. Additionally, the mass balance developed for a 50 L formulation batch was used as the basis for estimating direct production costs. Under these conditions, the total energy demand was estimated at 10.70 kWh per batch. Considering an average commercial electricity tariff of 0.25 USD kWh^{-1} in Costa Rica, the corresponding energy cost was estimated at 2.67 USD per batch.

The distribution of energy consumption among process units is presented in Table 3. The largest contributions correspond to raceway operation (34.3%), emulsification (34.6%), and intermittent aeration (21.0%), which together account for approximately 90% of the total energy

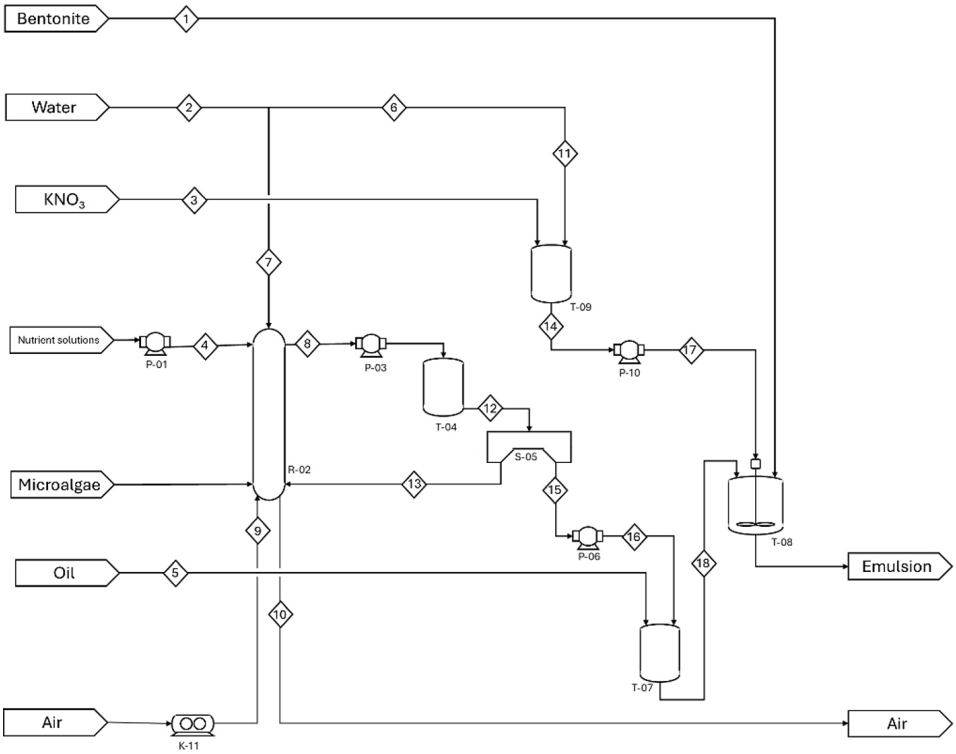

Figure 15. Flow diagram of the emulsion formation process

Table 4. Main process streams considered in the process flow diagram (PFD) formulation tank

Stream	Description	Basis	Value
F-01	Broth harvested from raceway to buffer tank	Per harvest	0.3 m³
F-02	Dry biomass contained in F-01	Per harvest	0.623 kg
F-03	Fraction of broth sent to centrifuge	Per emulsion tank	0.128 m³
F-04	Wet biomass at centrifuge outlet	Per emulsion tank	1.47 kg
F-05	Dry biomass contained in F-04	Per emulsion tank	0.250 kg
F-06	Water contained in F-04	Per emulsion tank	1.22 kg
F-07	Centrifuge clarified stream	Per emulsion tank	0.126 m³ minus separated wet biomass
F-08	Fresh water to mixing tank	Per emulsion tank	23.78 L
F-09	Oil to mixing tank	Per emulsion tank	25.000 L
F-10	KNO_3 to aqueous phase	Per emulsion tank	0.129 kg
F-11	Bentonite to aqueous phase	Per emulsion tank	2 kg
F-12	Oil + wet biomass stream to emulsification	Per emulsion tank	oil = 25.000 L; wet biomass = 1.47 kg
F-13	Final emulsion to T-13	Per tank	50 L
F-14	Dry biomass in final emulsion	Per tank	0.250 kg

demand. Centrifugation represents an intermediate contribution, whereas the transfer pumps account for only a minor fraction of the overall consumption.

The energy demand associated with emulsification is consistent with the rheological behavior of the formulated product. The Herschel–Bulkley model revealed shear-thinning behavior, characterized by a reduction in apparent viscosity at high shear rates, facilitating mixing and pumping operations. Simultaneously, the yield stress contributes to maintaining stability under low-shear conditions, reducing phase separation during storage (Chalah et al., 2025). Consequently, future optimization efforts should focus primarily on raceway recirculation, aeration, emulsification, and centrifugation, as these stages represent the main opportunities for reducing operational energy requirements.

CONCLUSIONS

The MATLAB-based model successfully simulated microalgal biomass production in the raceway system, with a predicted annual production of 606.26 kg year^{-1}, closely matching the reference value of 610.5 kg year^{-1} and showing consistency with the performance reported for the Almería University raceway system. The close agreement between these results verification the computational approach and demonstrates its suitability for predicting biomass production and supporting the subsequent design and scale-up of the pilot-scale system.

The developed Pickering emulsion demonstrated promising potential as a stable and effective delivery system for microalgae-based agricultural biostimulants. *Scenedesmus* sp. exhibited a half-life of 145 days in corn oil, highlighting its potential for long-term preservation. Fluorescence microscopy confirmed the presence of microalgal cells both in the continuous aqueous phase and associated with dispersed oil droplets. Furthermore, the emulsion exhibited biostimulant activity across all evaluated protocols, outperforming the application of microalgae alone at an equivalent dose, with a 200% increase in germination index compared to the positive control. Overall, these findings support the potential of Pickering emulsions as promising formulations for microalgal preservation, storage, transport, and agricultural applications.

The formulation system was successfully optimized and validated, demonstrating the influence of the operating conditions on Pickering emulsion stability. The factorial analysis showed that the relative contribution of agitation speed, mixing time, and draft tube configuration varied with storage time, supporting the selection of 2000 rpm and 10 min as the operating conditions for subsequent scale-up. Validation experiments confirmed the reproducibility of the formulation procedure, while the complementary two-way ANOVA showed that mixing time, draft tube configuration, and their interaction significantly affected stability when longer mixing times were evaluated. Rheological characterization of the selected formulation revealed a yield-stress, shear-thinning behavior accurately described by the Herschel–Bulkley model, providing a favorable balance between stability under low-shear conditions and processability at high shear rates. Together, these results support the robustness of the formulation system and provide the experimental and rheological basis required for its scale-up.

REFERENCES

1. BDO Costa Rica. (2025, December 22). *Costa Rica: ajuste en cuotas obrero–patronales de la CCSS a partir del 1.º de enero de 2026*. https://www.bdo.cr/es-cr/publicaciones/2025/costa-rica-ajuste-en-cuotas-obrero-patronales-de-la-ccss-a-partir-del-1-de-enero-de-2026
2. Bernal-Samaniego, C. (2021). *Establecimiento de un bioformulado en emulsión a base de microalgas para su uso en sistemas de producción agrícolas sostenibles*. Tecnológico de Costa Rica.
3. Calijuri, M. L., Silva, T. A., Magalhães, I. B., Pereira, A. S. A. de P., Marangon, B. B., Assis, L. R. de, Lorentz, J. F. (2022). Bioproducts from microalgae biomass: Technology, sustainability, challenges and opportunities. In *Chemosphere* (Vol. 305). Elsevier Ltd. https://doi.org/10.1016/j.chemosphere.2022.135508
4. Cerretelli, S., Castellanos, E., González-Mollinedo, S., Lopez, E., Ospina, A., Haggar, J. (2023). A scenario modelling approach to assess management impacts on soil erosion in coffee systems in Central America. *Catena*, *228*(April). https://doi.org/10.1016/j.catena.2023.107182
5. Chalah, K., Hammiche, D., Bennnoui, I.,

Benmounah, A. (2025). Evaluation of shear yield stress and apparent viscosity of xanthan gum solutions: application of rheological models and analytical study. *Macromolecular Research*, *33*(4), 423–437. https://doi.org/10.1007/s13233-024-00346-7

6. Costache, T. A., Gabriel Acien Fernandez, F., Morales, M. M., Fernández-Sevilla, J. M., Stamatin, I., Molina, E. (2013). Comprehensive model of microalgae photosynthesis rate as a function of culture conditions in photobioreactors. *Applied Microbiology and Biotechnology*, *97*(17), 7627–7637. https://doi.org/10.1007/s00253-013-5035-2
7. Covell, L., Machado, M., Vaz, M. G. M. V., Soares, J., Batista, A. D., Araújo, W. L., Martins, M. A., Nunes-Nesi, A. (2020). Alternative fertilizer-based growth media support high lipid contents without growth impairment in Scenedesmus obliquus BR003. *Bioprocess and Biosystems Engineering*, *43*(6), 1123–1131. https://doi.org/10.1007/s00449-020-02301-
8. EL Mernissi, N., EL Arroussi, H. (2024). Biofertilizers, soil conditioners, and biostimulants from microalgae. *Algal Bioreactors: Science, Engineering and Technology of Upstream Processes: 1,* 1, 593–602. https://doi.org/10.1016/B978-0-443-14058-7.00042-7
9. Fernández, I., Acién, F. G., Guzmán, J. L., Berenguel, M., Mendoza, J. L. (2016). Dynamic model of an industrial raceway reactor for microalgae production. *Algal Research*, *17*, 67–78. https://doi.org/10.1016/j.algal.2016.04.021
10. Ferreira, A., Corrêa, D. O., Ribeiro, B., Lopes da Silva, T., Marques-dos-Santos, C., Gabriel Acién, F., Gouveia, L. (2024). Bioprocess to produce biostimulants/biofertilizers based on microalgae grown using piggery wastewater as nutrient source. *Bioresource Technology*, *414*. https://doi.org/10.1016/j.biortech.2024.131619
11. Gao, S., Edmundson, S., Huesemann, M. (2022). Oxygen stress mitigation for microalgal biomass productivity improvement in outdoor raceway ponds. *Algal Research*, *68*, 102901. https://doi.org/10.1016/J.ALGAL.2022.102901
12. Ge, X. hui, Mo, L., Yu, A., Tian, C., Wang, X., Yang, C., Qiu, T. (2022). Stimuli-responsive emulsions: Recent advances and potential applications. *Chinese Journal of Chemical Engineering*, *41*, 193–209. https://doi.org/10.1016/j.cjche.2021.11.002
13. Gonçalves, J., Freitas, J., Fernandes, I., Silva, P. (2023). Microalgae as Biofertilizers: A Sustainable Way to Improve Soil Fertility and Plant Growth. *Sustainability (Switzerland)*, *15*(16), 1–19. https://doi.org/10.3390/su151612413
14. González-Hernández, J., Guzmán, J. L., Úbeda, J. C. M., Acién, F. G. (2024a). A graphical simulation tool to estimate microalgae production capacity around the world. *Algal Research*, *83*, 103665. https://doi.org/10.1016/J.ALGAL.2024.103665
15. González-Hernández, J., Guzmán, J. L., Úbeda, J. C. M., Acién, F. G. (2024b). A graphical simulation tool to estimate microalgae production capacity around the world. *Algal Research*, *83*(May). https://doi.org/10.1016/j.algal.2024.103665
16. González-Hernández, J., Guzmán, J. L., Úbeda, J. C. M., Acién, F. G. (2024c). A graphical simulation tool to estimate microalgae production capacity around the world. *Algal Research*, *83*. https://doi.org/10.1016/j.algal.2024.103665
17. Guzmán, J. L., Rodríguez-Miranda, E., Berenguel, M., Acién, F. G., García-Gallardo, J. (2025a). A Web-Based Virtual Lab for Microalgae Raceway Photobioreactors: Enhancing Modeling and Control Education. *IFAC-PapersOnLine*, *59*(7), 36–41. https://doi.org/10.1016/j.ifacol.2025.08.019
18. Guzmán, J. L., Rodríguez-Miranda, E., Berenguel, M., Acién, F. G., García-Gallardo, J. (2025b). A web-based virtual lab for microalgae raceway photobioreactors: enhancing modeling and control education. *IFAC-PapersOnLine*, *59*(7), 36–41. https://doi.org/10.1016/j.ifacol.2025.08.019
19. IFPRI. (2026). *Toward sustainable agricultural development in Costa Rica | IFPRI*. (2007), 543–562.
20. Jeon, T. Y., Hong, J. S. (2014). Stabilization of O/W emulsion with hydrophilic/hydrophobic clay particles. *Colloid and Polymer Science*, *292*(11), 2939–2947. https://doi.org/10.1007/s00396-014-3353-2
21. Jeong, S. W., Locat, J., Leroueil, S. (2012). The effects of salinity and shear history on the rheological characteristics of illite-rich and na-montmorillonite-rich clays. *Clays and Clay Minerals*, *60*(2), 108–120. https://doi.org/10.1346/CCMN.2012.0600202
22. Kusvuran, A., Can, A. G. (2020). Effects of microalga (*Chlorella vulgaris* beijerinck) on seconder metabolites and antioxidative defense system improve plant growth and salt tolerance in guar [*Cyamopsis tetragonoloba* (L.) taub.]. *Legume Research*, *43*(1), 56–60. https://doi.org/10.18805/LR-492
23. Kusvuran, A., Kusvuran, S. (2019). Using of Microbial Fertilizer as Biostimulant Alleviates Damage from Drought Stress in Guar (*Cyamopsis Tetragonoloba* (L.) Taub.) Seedlings. *International Letters of Natural Sciences*, *76*, 147–157. https://doi.org/10.18052/www.scipress.com/ilns.76.147
24. Kusvuran, S. (2021). Microalgae (*Chlorella vulgaris* Beijerinck) alleviates drought stress of broccoli plants by improving nutrient uptake, secondary metabolites, and antioxidative defense system. *Horticultural Plant Journal*, *7*(3), 221–231. https://doi.org/10.1016/j.hpj.2021.03.007
25. Navarro-López, E., Ruíz-Nieto, A., Ferreira, A., Gabriel Acién, F., Gouveia, L. (2020). Biostimulant

potential of scenedesmus obliquus grown in brewery wastewater. *Molecules*, *25*(3). https://doi.org/10.3390/molecules25030664

26. Ou, L., Zhuang, H., Chen, R., Lei, J., Liao, X., Lin, W. (2007). Methods on observation of fluorescence micro-imaging for microalgae. *Optics in Health Care and Biomedical Optics III*, *6826*, 68262P. https://doi.org/10.1117/12.756970
27. Peters, M. S., Timmerhaus, K. D. (1991). Plant and design economics for chemical engineers. In *Plant design and economics for chemical engineers*.
28. Qi, L., Hang, T., Jiang, W., Li, S., Zhang, H., Liang, X., Lei, L., Bi, Q., Jiang, H., Li, Y. (2024). Proteinaceous microsphere-based water-in-oil pickering emulsions for preservation of chlorella cells. *Polymers*, *16*(5). https://doi.org/10.3390/polym16050647
29. Rodríguez-Mora, K., Villlalta-Romero, F., Nuñez-Salazar, Y., Ossa, A., Montero, M. L. (2026a). Evaluation of the biostimulant activity of the microalgae *Chlorella sorokiniana* and *Scenedesmus* sp. and their resistance to the most widely used agricultural pesticides. *ACS Omega*, *11*(20), 29541–29549. https://doi.org/10.1021/acsomega.5c11935
30. Rodríguez-Mora, K., Montero, M., Hernández-Varela, J.D., Chanona-Pérez, J.D., Ramírez-Ortiz, M.E. (2026b). Harnessing nanoclays: optimizing sustainable Pickering emulsions with bentonite and kaolin nanoparticles. *Clays and Clays Minerals.*
31. Rogers, J. N., Rosenberg, J. N., Guzman, B. J., Oh, V. H., Mimbela, L. E., Ghassemi, A., Betenbaugh, M. J., Oyler, G. A., Donohue, M. D. (2014a). A critical analysis of paddlewheel-driven raceway ponds for algal biofuel production at commercial scales. *Algal Research*, *4*(1), 76–88. https://doi.org/10.1016/J.ALGAL.2013.11.007
32. Rogers, J. N., Rosenberg, J. N., Guzman, B. J., Oh, V. H., Mimbela, L. E., Ghassemi, A., Betenbaugh, M. J., Oyler, G. A., Donohue, M. D. (2014b). A critical analysis of paddlewheel-driven raceway ponds for algal biofuel production at commercial scales. *Algal Research*, *4*(1), 76–88. https://doi.org/10.1016/J.ALGAL.2013.11.007
33. Ronga, D., Biazzi, E., Parati, K., Carminati, D., Carminati, E., Tava, A. (2019). Microalgal biostimulants and biofertilisers in crop productions. *Agronomy*, *9*(4), 1–22. https://doi.org/10.3390/agronomy9040192
34. Safi, C., Zebib, B., Merah, O., Pontalier, P. Y., Vaca-Garcia, C. (2014). Morphology, composition, production, processing and applications of *Chlorella vulgaris*: A review. *Renewable and Sustainable Energy Reviews*, *35*, 265–278. https://doi.org/10.1016/j.rser.2014.04.007
35. Sánchez-zurano, A., Rodríguez-miranda, E., Guzmán, J. L., Acién-fernández, F. G., Fernández-sevilla, J. M., Grima, E. M. (2021). Abaco: A new model of microalgae-bacteria consortia for biological treatment of wastewaters. *Applied Sciences (Switzerland)*, *11*(3), 1–24. https://doi.org/10.3390/app11030998
36. Song, X., Liu, J., Feng, Y., Zhou, C., Li, X., Yan, X., Ruan, R., Cheng, P. (2024). Microalgae-based biofertilizers improve fertility and microbial community structures in the soil of potted tomato. *Frontiers in Plant Science*, *15*(December), 1–12. https://doi.org/10.3389/fpls.2024.1461945
37. Sun, Z., Yan, X., Xiao, Y., Hu, L., Eggersdorfer, M., Chen, D., Yang, Z., Weitz, D. A. (2022). Pickering emulsions stabilized by colloidal surfactants: Role of solid particles. *Particuology*, *64*, 153–163. https://doi.org/10.1016/j.partic.2021.06.004
38. Tadros, T. F. (2013). Emulsion formation, stability, and rheology. *Emulsion Formation and Stability*, 1–75. https://doi.org/10.1002/9783527647941.ch1
39. Vangenechten, B., De Coninck, B., Ceusters, J. (2025). How to improve the potential of microalgal biostimulants for abiotic stress mitigation in plants? *Frontiers in Plant Science*, *16*(April). https://doi.org/10.3389/fpls.2025.1568423
40. Varela-Benavides, I., Jiménez-Madrigal, J. P., Echeverría-Beirute, F., Castro-Jiménez, Z. (2022). Nematode communities in pineapple plantations in the plains of the Región Huetar Norte, Costa Rica. *Nematropica*, *52*(1), 19–32.
41. Vildanova, G. I., Allaguvatova, R. Z., Kunsbaeva, D. F., Sukhanova, N. V., Gaysina, L. A. (2023). Application of *Chlorella vulgaris* Beijerinck as a biostimulant for growing cucumber seedlings in hydroponics. *BioTech*, *12*(2), 42. https://doi.org/10.3390/biotech12020042
42. Villalta-romero, F., Murillo-vega, F., Martínez-gu-, B. (2019). Microalgal biotechnology in Costa Rica : Business opportunities to the national productive sector Biotecnología microalgal en Costa Rica : Oportunidades de negocio para el sector productivo nacional. *Tecnología en Marcha, 32*, 85–93.
43. Wang, X., Alvarado, V. (2011). Kaolinite and silica dispersions in low-salinity environments: Impact on a water-in-crude oil emulsion stability. *Energies*, *4*(10), 1763–1778. https://doi.org/10.3390/en4101763
44. Zhai, M., Zhou, K., Sun, Z., Xiong, Z., Du, Q., Zhang, Y., Shi, L., Hou, J. (2023). Rheological characterization and shear viscosity prediction of heavy oil-in-water emulsions. *Journal of Molecular Liquids*, *381*, 121782. https://doi.org/10.1016/j.molliq.2023.121782